The Moon Illusion and Size–Distance Scaling—Evidence for Shared Neural Patterns

Ralph Weidner[1*], Thorsten Plewan[1,2*], Qi Chen[1], Axel Buchner[3], Peter H. Weiss[1,4], and Gereon R. Fink[1,4]

Abstract

■ A moon near to the horizon is perceived larger than a moon at the zenith, although—obviously—the moon does not change its size. In this study, the neural mechanisms underlying the "moon illusion" were investigated using a virtual 3-D environment and fMRI. Illusory perception of an increased moon size was associated with increased neural activity in ventral visual pathway areas including the lingual and fusiform gyri. The functional role of these areas was further explored in a second experiment. Left V3v was found to be involved in integrating retinal size and distance information, thus indicating that the brain regions that dynamically integrate retinal size and distance play a key role in generating the moon illusion. ■

INTRODUCTION

Although the moon does not change its size, the moon near to the horizon is perceived as relatively larger compared with when it is located at the zenith. This phenomenon is called the "moon illusion" and is one of the oldest visual illusions known (Ross & Plug, 2002). Despite extensive research, no consensus has been reached regarding the underlying perceptual and neural correlates (Ross & Plug, 2002; Hershenson, 1989).

Many researchers agree that the moon illusion is caused by mechanisms that otherwise allow an accurate perception of an object's size, regardless of its distance (size constancy). However, there are different opinions on how size scaling and size constancy are implemented in the human visual system.

For instance, Berkeley (1709/1948) suggested that size scaling is achieved by taking into account learned proprioceptive and visual cues such as the angle of regard or aerial perspective. It has furthermore been proposed that constant size representations are formed by taking into account the relative size of neighboring objects (Baird, Wagner, & Fuld, 1990; McCready, 1986; Restle, 1970; Rock & Ebenholtz, 1959), texture gradients, and invariant properties of the environment (Gibson, 1979; please see Ross & Plug, 2002; Ross & Plug, 1998, for more elaborated reviews). In addition, perceived size has been linked to oculomotor processes such as accommodation (accommodative micropsia) and convergence (convergence micropsia; Sperandio, Kaderali, Chouinard, Frey, & Goodale, 2013; Enright, 1989; Roscoe, 1989).

One concept of size constancy scaling implies that the retinal image size and the estimated distance of an object are conjointly considered, thereby enabling constant size perception of objects at different distances (Kaufman & Kaufman, 2000). With respect to the moon illusion, apparent distance theories, for example, propose that "the perceived distance to the moon at the horizon is greater than to the zenith moon" (Kaufman & Kaufman, 2000), and therefore, despite the constant retinal size, the horizontal moon generates a larger percept than the zenithal moon.

One of many problems with this interpretation is, however, that participants tend to report the horizontal moon as both larger and nearer (Hershenson, 1989), a phenomenon commonly referred to as the size–distance paradox. A potential solution of this paradox is to postulate the existence of different levels of distance representations in the brain (i.e., registered distance and apparent distance). According to this view, size distance scaling is initially based on one form of distance representation (e.g., registered distance), which makes the moon appear larger. This larger appearance then reduces "apparent" distance, which results in the moon appearing closer (Gogel & Mertz, 1989; Rock & Kaufman, 1962).

Likewise, the neural mechanisms underlying the moon illusion are unclear. Different variants of apparent distance theories consistently suggest that the moon illusion involves brain areas that integrate distance and retinal (angular) object size to generate size–distance invariant object representations.

Thus far, investigating the "natural" moon illusion within an fMRI setting was hindered by the fact that the moon cannot easily be transferred to an artificial environment.

[1]Research Centre Jülich, [2]Leibniz Research Centre for Working Environment and Human Factors (IfADo), Dortmund, Germany, [3]Heinrich-Heine-Universität Düsseldorf, [4]Cologne University
*These authors contributed equally to this work.

Journal of Cognitive Neuroscience 26:8, pp. 1871–1882
doi:10.1162/jocn_a_00590

For instance, binocular vision seems to play an important role in enhancing the apparent size of the nearby horizon moon (e.g., Enright, 1989). Presenting the moon illusion on a standard 2-D computer screen may thus obscure important aspects. Nowadays, however, visual stimulus presentation devices such as magnetic resonance (MR)-compatible goggle systems allow 3-D presentation even within an fMRI environment, thereby enabling a functional investigation of the moon illusion, albeit an artificial one.

The goal of this study was not only to reveal the neural correlates associated with experiencing this illusion by transferring the moon illusion into an fMRI suitable setting but also to relate the neural correlates underlying the moon illusion to those linked to different levels of object size perception.

To identify the neural network underlying the moon illusion and to delineate different levels of visual processing represented within such a network, two fMRI experiments were performed: The first experiment directly investigated the neural activity related to the moon illusion by presenting computer-generated (binocular) 3-D stimuli of a virtual moon at two different positions (low or high), either within a natural scene or on a neutral background resulting in a two factorial design (see Figure 1A). Brain regions underlying the moon illusion were expected to be revealed by an interaction between the factors moon position (low vs. high) and scene (with or without). More specifically, the perceived size of the virtual moon was expected to be increased only at the lower position in combination with the presence of a scene.

A second experiment was performed to test whether the moon illusion is generated by brain regions that form size-invariant (linear) object representations by taking into account retinal (angular) size and perceived distance. Such brain regions were identified by means of fMRI adaptation (Grill-Spector & Malach, 2001). Participants saw spheres located in different depth planes, with either constant or variable perceived size (see Figure 1B). The latter was realized by altering the perceived distance between observer and object while simultaneously keeping the object's retinal (angular) size constant.

METHODS

Participants

Twenty-five healthy participants (12 women) participated in a single fMRI session consisting of two separate experiments. All participants were paid for their participation and gave informed consent before the experiments in accordance to the declaration of Helsinki. The study was approved by the ethics committee of the German Society of Psychology. Participants' ages ranged from 19 to 39 years with a mean age of 29.4 (SD = 6.04).

All participants had normal or corrected-to-normal vision during the experiment.

fMRI Measurement and Data Preprocessing

Functional imaging data were acquired by means of a 3-T TRIO MRI system (Siemens, Erlangen, Germany) using T2*-weighted EPI sequence (repetition time = 2.2 sec, echo time = 30 sec). In Experiment 1, 415 volumes were acquired, and 605 volumes were obtained in Experiment 2. Each volume consisted of 36 axial slices, allowing for whole-brain coverage (3 mm thickness, distance factor 10%, field of view 200 mm, 64 × 64 matrix, in-plane voxel size 3 × 3 mm^2).

The fMRI data preprocessing and statistical inference were performed using the Statistical Parametric Mapping software (Friston et al., 1994). The first four images were excluded from the analysis, as these were acquired within the time period the MR signal needs to reach a steady state. Images were spatially realigned to the fifth volume to correct for interscan movement. Then the mean EPI image for each participant was computed and spatially normalized to the Montreal Neurological Institute (MNI) template using the "unified segmentation" function in SPM5 (Ashburner & Friston, 2005). The data were then smoothed using a Gaussian kernel of 8 mm FWHM.

EXPERIMENT 1: MOON ILLUSION

Stimuli

Visual stimuli were presented using an MR-compatible 3-D goggle system (VisuaStim, Resonance Technology, Northridge, CA). The device consists of two thin-film transistor (TFT) displays with a screen diagonal of 37.5° visual angle. The stimuli that covered the whole display were presented as disparate images on the two TFT displays of the binocular goggles and hence generated a marked depth impression. The stimulus background consisted of either an artificial scene (henceforth "with scene") or alternatively of a plain blue screen (henceforth "without scene"; see Figure 1A). Orthogonal to the scene variable, a small moon (0.83° visual angle) appeared at one of the two possible positions (low or high). Hence, the experiment was based on a 2 × 2 factorial design with Scene (with vs. without) and Moon Position (low vs. high) as within-subject variables. A behavioral pilot experiment (data not shown) had confirmed that this setting is appropriate for reliably inducing the moon illusion.

Throughout this fMRI experiment, two white bars were presented continuously on the left and on the right margin of the screen, which served as background for a comparison disk that was superimposed either on the left or on the right bar. Its vertical position was set between the two possible moon positions (see Figure 1A).

Task and Design

Participants were instructed to indicate via button press whether the comparison disk was perceived as being smaller or larger than the moon presented in the display.

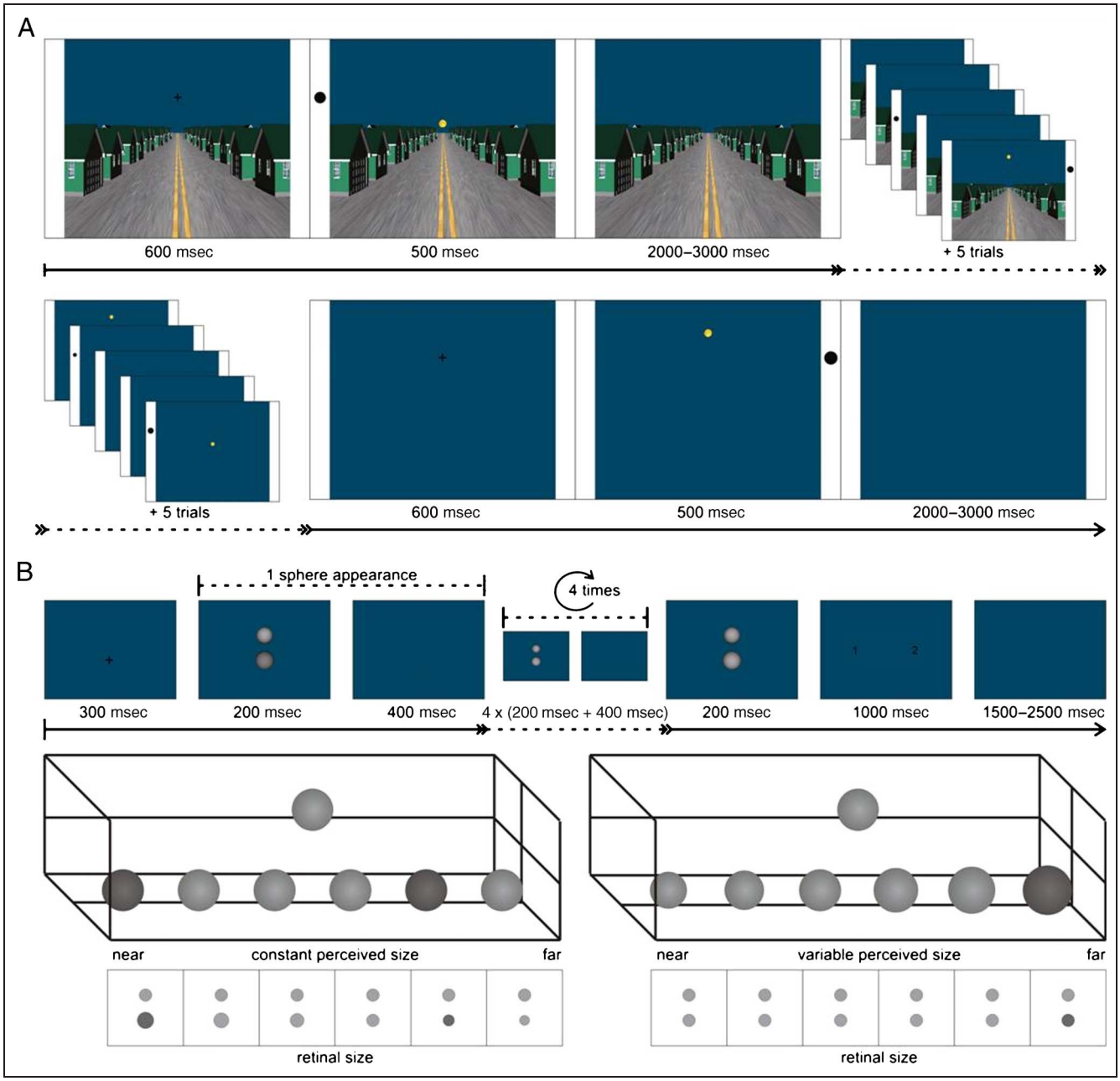

Figure 1. Overview of the experimental conditions. (A) Experiment 1: Moon illusion. The upper row depicts an example miniblock of the "with scene" condition. A trial consisted of a fixation period, an experimental period, and an intertrial interval; six trials comprised a miniblock (top right). The bottom row illustrates the "without scene" condition. The moon appeared randomly either in low or high position. At the same time participants had to decide whether the comparison disk in the white framing bars was smaller or bigger than the moon. (B) Experiment 2: Size constancy. The upper row sketches a possible trial. A short fixation period was followed by six appearances of the spheres, while each appearance was parted by a short blank screen period (indicated by dotted line segment). Trials were terminated by an answer screen and the variable intertrial interval. In this example, the lower sphere is variable, whereas the upper is kept constant throughout the trial in terms of color (light gray) and position in depth. As depicted, the variable sphere could appear either in dark or light gray while it changed its position in depth. Middle row: Positions in depth and perceived sizes of the spheres for both experimental conditions are illustrated. For illustrative purposes, the figures show side views into a 3-D space, please note that participants had a frontal view (i.e., from the left end of the figures). Bottom row: Retinal images used to induce the described (depth) perceptions.

Initially the diameter of the comparison disk was set either to a clearly smaller or larger size than the moon. Depending on the participant's responses, the diameter of the comparison disk was changed on a trial-by-trial basis according to an adaptive algorithm called "parameter estimation by sequential testing" (Taylor & Creelman, 1967).

Experiment 1 consisted of 240 trials, half of which were with scene and half were without.

In half of the trials, the moon was presented at the lower position and in half of the trials at a higher position. At each level of the scene variable (scene present, scene absent), one third of the trials were replaced by null

events. Thus, there were 40 trials in each condition as well as 40 null event trials with scene and 40 without scene. To maintain a stable depth perception, stimuli were presented in miniblocks of six trials. The sequence in which the conditions were presented was randomized across participants.

Pilot testing had shown that 20 trials were sufficient to arrive at a stable size estimate within a particular condition. Thus, the size of the comparison disk was saved at the end of the 20th trial in each condition and then reset to an initial value (if the first size estimation started with a small diameter, then the second size estimation was initiated with a larger one and vice versa). Following this procedure, it was possible to obtain two size estimations from each participant for each condition, which were then averaged.

A trial started with a fixation cross presented for 600 msec, which was vertically positioned between the two possible locations of the virtual moon. Subsequently, the virtual moon was presented for 500 msec, and the participant's response was recorded. Each trial was terminated by a randomly selected intertrial interval of 2000, 2500, or 3000 msec following the presentation of the virtual moon.

fMRI Data Analysis

Five participants had to be excluded from the functional analysis, leaving a sample of 20 participants (10 women): Two participants extensively moved during the scanning session (>3 mm), technical problems with the MR scanner stopped the scanning procedure for one participant, for another participant the recording of the experimental data was erroneous, and one participant was unable to finish the session because of dizziness.

To be able to test for a significant interaction of both main factors, four regressors of interest were defined reflecting the cells of the 2 × 2 factorial design with Moon Position (low vs. high) and Scene (with vs. without) as within-subject variables. In particular, onsets were defined as the time of occurrence of the moon. Each occurrence was considered as a single event.

Trials with more or less than exactly one answer (button press) were considered erroneous and were therefore not included in any regressor. Furthermore, additional regressors including parametric modulations representing the size of the comparison disk diameter were included. The hemodynamic response to each type of event was modeled using a canonical synthetic hemodynamic response function and its first derivative. The six head-movement parameters were included as confounds and nonsphericity correction was applied where appropriate.

First-level linear baseline contrasts were calculated comparing the four regressors of interest with the implicit baseline (i.e., those time periods that were not explicitly modeled and in which no event occurred). These contrasts were then taken to the second level, where they were subjected to a repeated-measures ANOVA with moon position (low, high) and the scene (with, without scene), using a corrected threshold (family wise error correction [FWE]) of $p < .01$ at the cluster level ($p < .001$ cut-off at the voxel level).

EXPERIMENT 2: SIZE CONSTANCY

Stimuli

Stimuli were presented via 3-D goggles (see Experiment 1 for details). Binocular stimulus presentation allowed generating a marked depth impression. It is known that stereoscopic depth perception relies mainly on relative disparity, that is, disparity differences, rather than on absolute disparity values (Neri, Bridge, & Heeger, 2004). Hence, to evoke a more pronounced depth impression, two gray-colored spheres were presented simultaneously on a blue background with the spheres located below and above the screen center (see Figure 1B). While one of the spheres was static, the other sphere changed its position in depth and its relative size.

The vertical position of a fixation cross served as a precue and consistently indicated the position of the sphere that would vary in depth (i.e., whether it would be the upper or lower sphere that varies in depth). The position of this variable sphere was counterbalanced across conditions. Generally, the variable sphere was presented at six different positions in depth, starting either from the back moving toward the front or vice versa. In two different conditions, these depth changes went along with either changes in perceived or in retinal size. To keep retinal size constant, the sphere subtended a visual angle of 3.99° at each position in space. To keep the perceived size constant, the sphere changed its size in terms of visual angle as a function of its position in depth (ranging continuously between 2.49° visual angle in far position and 5.5° visual angle in near position). The constant sphere was at a medium depth position between the near and far endpoints. It subtended a visual angle of 3.54°. Within each course of a trial, either one or two changes in luminance were assigned to the variable sphere (see Figure 1B).

Task and Design

fMRI adaptation makes use of the principle that the responses of a neuron elicited by consecutive presentation of the same evocative stimulus or event decay over time. However, changing the properties of the evocative event (i.e., making it another kind of stimulus or event), activates a different population of neurons, consequently evoking a nonattenuated neural response. This paradigm has been used successfully in fMRI studies to delineate functional properties of neural representations (Grill-Spector & Malach, 2001). Experiment 2 was designed to make use of the fMRI adaptation paradigm to identify

areas subserving different levels of object size perception within a 3-D context. To delineate processing stages that alter the perceived size of an object and those constantly coding object size in a distance-invariant (perceived) manner, either the perceived or the retinal size of a stimulus was varied along with changes in perceived depth.

The first condition aimed at identifying areas responding when the perceived size of an object was changed. Therefore, the retinal size of an object, presented at different distances, was kept constant, generating variations of the perceived size (henceforth referred to as "variable perceived size condition"). Brain regions responding to changes of the perceived size of an object were expected to adapt in consecutive trials.

In the second condition, changes in depth were associated with changes in retinal size such that object size was perceived as constant across different distances (henceforth referred to as "constant perceived size condition"). Brain areas coding constant perceived object size were expected to respond invariantly across different distances, and hence following the logic of the fMRI adaptation paradigm, these areas should adapt and respond weaker in subsequent trials.

Experiment 2 consisted of 200 trials. Following a fixation cross (300 msec), the spheres appeared six times sequentially (200 msec each) with an ISI of 400 msec. After the last sphere had been presented, a screen appeared (1000 msec), which prompted the participants to respond. To keep participants' attention focused on the stimuli, participants were asked to perform a luminance change detection task. The task was to indicate the number of luminance changes within a trial via a button press (index finger = 1, middle finger = 2). The occurrence of one or two changes per trial was equally likely. To maintain high alertness across each trial, the second of the two changes in the two-change trials occurred at the end of the trial. More precisely, with a probability of .9, the second change occurred while the variable sphere was at the last position or at the next to last position.

A trial was followed by an intertrial interval of 1500, 2000, or 2500 msec. Overall, there were 40 trials for each condition (constant perceived size vs. variable perceived size) in each direction (near to far vs. far to near). The upper sphere was variable in 20 of these trials, and the lower sphere was variable in the remaining 20 trials. Additionally, there were 40 null events in which only the fixation cross appeared. Type of trial as well as the direction and the position of the variable sphere were counterbalanced across the experiment.

fMRI Data Analysis

Eight participants had to be excluded from the analysis, leaving a sample of 17 participants (7 women): Five participants moved during the scanning procedure (>3 mm). The scanning session of two participants had to be stopped because of technical problems, and one participant was not able to finish the session because of dizziness.

Overall, six onset regressors were defined. Separately for the constant and the variable perceived size conditions, trials were subdivided into "adapt" and "new" trials, depending on whether or not they were preceded by the same or the other condition (resulting in four regressors of interest). As mentioned above, if a constant perceived size trial was preceded by another constant perceived size trial, it was assigned to the "adapt" trial set, whereas a constant perceived size trial that was preceded by a variable perceived size trial was assigned to the "new" set. Likewise, the variable perceived size trials were assigned to different groups. In addition, a (fifth) regressor for error trials (except for one participant who performed the task without any mistakes) and a (sixth) regressor for the answer period were explicitly defined. The first appearance of a sphere within a trial was defined as onset time and trial duration was specified as 3.2 sec. Duration of the answer period was 1 sec and started with the onset of the answer screen.

The hemodynamic response to each type of event was modeled using a canonical synthetic hemodynamic response function and its first derivative. The six head movement parameters were included as confounds and nonsphericity correction was employed when needed. First-level linear baseline contrasts were calculated comparing the regressors of interest with the implicit baseline. These contrasts were then taken to the second level, where they were subjected to a repeated-measures ANOVA with one factor, namely Adaptation ("new" vs. "adapt").

Given that the rational of the second experiment was to test whether the brain regions contributing to the moon illusion either code constant perceived size or changes of the perceived size, the analysis was restricted to those voxels that showed a significant interaction between moon position and scene in Experiment 1. This was achieved by generating a binary mask based on the voxels (interaction contrast) activated in Experiment 1, which then served as an implicit mask for the analysis. Accordingly, a corrected threshold of $p < .05$ (FWE, extend threshold 5 voxels) was applied.

ROI Analysis

The relationship between the BOLD signal and behavior was further investigated using an ROI-based approach. Beta values representing estimates of BOLD signal amplitudes were extracted for each local maximum within a cluster of activation associated with the moon illusion. This was performed separately for each participant and for all four experimental conditions of Experiment 1.

To test whether perceived size generally predicted BOLD amplitudes in the different brain regions, the

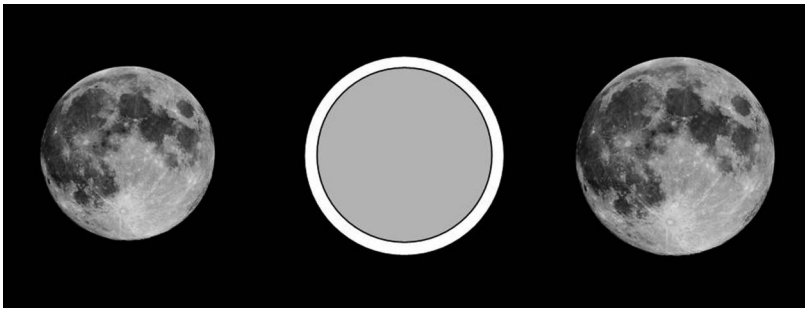

Figure 2. Illustration of the perceived size of the moon when increased by the moon illusion (right) relative to its physical size (left). The schematic circles in the middle display a direct overlay of both sizes and elucidate the perceived size difference.

estimates of perceived size were entered into simple linear regression analyses.

RESULTS

Behavioral

The strength of the moon illusion was measured using a size comparison task. This allowed estimating the perceived size of the moon separately for all four conditions, that is, at two different positions (low or high), either embedded into a scene or on a neutral background. As expected, the moon (actual size 0.83° visual angle) was perceived larger when presented near the horizon (0.95° visual angle, $SD = 0.09$) and smaller when presented at the higher position (0.92°, $SD = 0.09$), constituting a relative increase in perceived size by 3%. Furthermore, the moon was generally perceived smaller when the scene was absent (0.89°, irrespective of the moon's position) compared with when the moon was presented embedded into a scene (Figure 2). The effect of Scene on perceived moon size was supported by the results of a repeated-measures ANOVA, with Scene (with, without scene) and Moon Position (low, high) as within-subject variables. This analysis revealed a significant main effect of Scene, $F(1, 19) = 50.67$, $p < .01$, $\eta_p^2 = .73$, and a significant Scene × Moon Position interaction, $F(1, 19) = 4.41$, $p < .05$, $\eta_p^2 = .19$. Paired-sample t tests showed that, as predicted, there was a significant difference between the low and high moon position (i.e., a typical moon illusion) when a scene was present, $t(19) = 2.1$, $p < .05$, $d_z = 0.43$, whereas without a scene no such effect was observed, $t(19) = -0.13$, $p > .05$, $d_z = 0$.

Functional Data

Experiment 1

The brain regions underlying the moon illusion were revealed by an analogue analysis of the fMRI data. The relevant interaction contrast [(Moon low with scene–Moon high with scene)–(Moon low without scene–Moon high without scene)] revealed three significant clusters of activation (see Table 1A and Figure 3A). The strongest activation was located at the posterior aspect of the left fusiform gyrus (−44, −64, −14), extending posteriorly to the inferior temporal gyrus and superiorly into the calcarine sulcus. A second activation was located bilaterally

Table 1. Overview of fMRI Results

Brain Region	*Side*	*MNI Coordinates*			*Cluster Size*	*T Score*
A) Experiment 1: Moon Illusion						
Fusiform gyrus	L	−44	−64	−14	1669	5.69
Middle occipital gyrus (left V1)	L	−14	−100	0		4.88
Calcarine gyrus (right V1)	R	14	−96	−2	796	5.16
Fusiform gyrus	R	42	−40	−24	327	6.13
B) Experiment 2: Size Constancy						
Middle occipital gyrus	R	30	−88	2	79	5.34
Middle occipital gyrus	L	−24	−94	0	26	4.81

(A) List of activations reflecting the interaction between moon position and scene, that is, the effect of the moon illusion ($p < .01$, cluster level). The second coordinate (−14 −100 0) represents a submaximum of the larger cluster in the left hemisphere. All other coordinates represent cluster maxima. (B) List of activations related to the specific adaptation effects of constant retinal size, that is, variable perceived size ($p < .05$, FWE). All coordinates were defined within MNI space.

in early visual areas involving the right calcarine sulcus (14, −96, −2) and lingual gyrus as well as the left inferior and middle occipital gyrus. The third significant activation was located in the right fusiform gyrus (42, −40, −24). Brain areas involved in generating the moon illusion were expected to exhibit the strongest signal change in the moon low condition. Beta values (representing estimates of BOLD signal amplitudes) were extracted to confirm that the clusters which were significantly activated by the interaction term showed the predicted pattern of activity, that is, larger signal changes when the virtual moon was presented at the lower position within the context of the scene compared with its presentation at the high position. Moreover, the signal changes in both conditions with scene were larger than in the two control conditions without scene. The reverse whole brain interaction contrast did not reveal any significant activation [(Moon high with scene–Moon low with scene)–(Moon high without scene–Moon low without scene)].

Experiment 2

The second experiment aimed at identifying brain regions associated with different levels of object size coding by means of an fMRI adaptation paradigm (Grill-Spector & Malach, 2001).

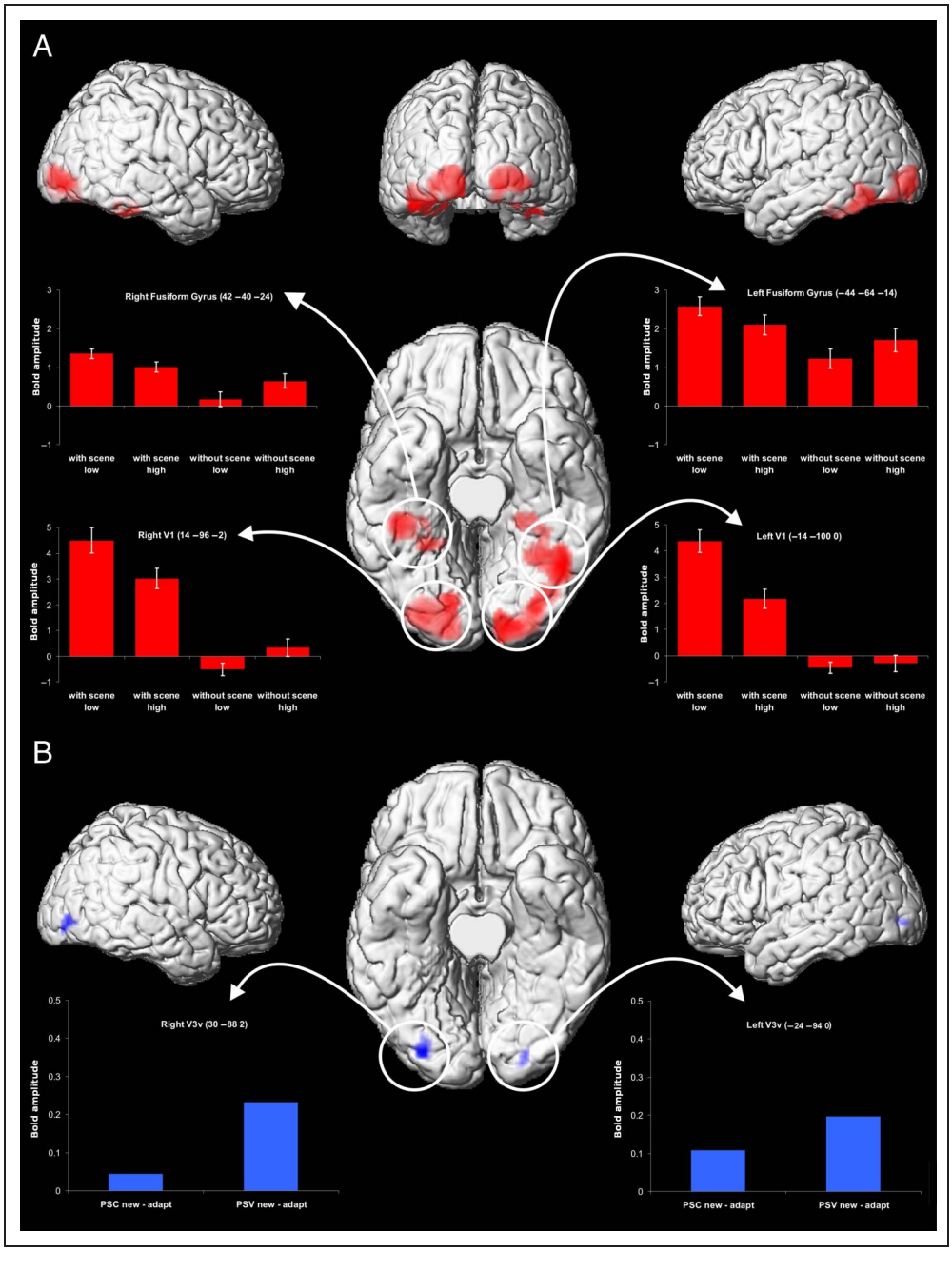

Figure 3. (A) Surface rendering and relative signal change values associated with the functional activations of the moon illusion (red). Arrows connect the particular brain region with its corresponding signal change pattern. The activation patterns were extracted from maximum activated voxels (see Table 1A) for all four experimental conditions. (B) Surface rendering related to the adaptation effect of variable perceived size (inclusively masked by activations from the moon illusion network, blue; see Table 1B). Arrows indicate the relative differences in signal change pattern between "new" and "adapt" trials (for both conditions: constant and variable perceived size). Differences were only significant in the variable size condition.

Table 2. Results of the Linear Regression Analyses Performed Separately for Different Regions and Separately for the Different Experimental Conditions

		Slope (Standardized)				*Variance*			
Region	*Condition*	*β*	*df*	*t Score*	*p Corrected*	r^2	*df*	*F Score*	*p Corrected*
Left V1	**Scene low**	**0.58**	**18**	**3.03**	***p* < .05**	**0.34**	**1, 18**	**9.18**	***p* < .05**
	Scene high	0.38	18	1.76	$p = .57$ *ns*	0.15	1, 18	3.11	$p = .57$ *ns*
	No scene low	0.53	18	2.68	$p = .09$ *ns*	0.29	1, 18	7.18	$p = .09$ *ns*
	No scene high	0.38	18	1.76	$p = .58$ *ns*	0.15	1, 18	3.09	$p = .576$ *ns*
Right V1	Scene low	0.49	18	2.36	$p = .18$ *ns*	0.24	1, 18	5.59	$p = .18$ *ns*
	Scene high	0.41	18	1.9	$p = .44$ *ns*	0.17	1, 18	3.6	$p = .44$ *ns*
	No scene low	0.39	18	1.77	$p = .56$ *ns*	0.15	1, 18	3.14	$p = .56$ *ns*
	No scene high	**0.61**	**18**	**3.24**	***p* < .05**	**0.37**	**1, 18**	**10.51**	***p* < .05**
Left fusiform	Scene low	0.16	18	0.68	$p = 1$ *ns*	0.03	1, 18	0.46	$p = 1$ *ns*
	Scene high	0.25	18	1.1	$p = 1$ *ns*	0.06	1, 18	1.2	$p = 1$ *ns*
	No scene low	0.05	18	0.22	$p = 1$ *ns*	0	1, 18	0.05	$p = 1$ *ns*
	No scene high	0.09	18	0.37	$p = 1$ *ns*	0.01	1, 18	0.14	$p = 1$ *ns*
Right fusiform	Scene low	0.26	18	1.14	$p = 1$ *ns*	0.07	1, 18	1.29	$p = 1$ *ns*
	Scene high	0.13	18	0.57	$p = 1$ *ns*	0.02	1, 18	0.33	$p = 1$ *ns*
	No scene low	0.15	18	0.64	$p = 1$ *ns*	0.02	1, 18	0.41	$p = 1$ *ns*
	No scene high	0.28	18	1.23	$p = 1$ *ns*	0.08	1, 18	1.52	$p = 1$ *ns*
Left V3v	**Scene low**	**0.66**	**18**	**3.73**	***p* < .05**	**0.44**	**1, 18**	**13.94**	***p* < .05**
	Scene high	0.5	18	2.47	$p = .14$ *ns*	0.25	1, 18	6.09	$p = .14$ *ns*
	No scene low	0.3	18	1.35	$p = 1$ *ns*	0.09	1, 18	1.84	$p = 1$ *ns*
	No scene high	0.43	18	2.03	$p = .35$ *ns*	0.19	1, 18	4.11	$p = .35$ *ns*
Right V3v	Scene low	0.53	18	2.62	$p < .10$ *ns*	0.28	1, 18	6.89	$p < .10$ *ns*
	Scene high	0.5	18	2.45	$p = .15$ *ns*	0.25	1, 18	5.99	$p = .15$ *ns*
	No scene low	0.15	18	0.66	$p = 1$ *ns*	0.02	1, 18	0.43	$p = 1$ *ns*
	No scene high	0.27	18	1.21	$p = 1$ *ns*	0.07	1, 18	1.45	$p = 1$ *ns*

Significant results, as indicated by a β (standardized slope) > 0 and significant *t* statistics, are highlighted in **bold**.

For both the constant and the variable perceived size conditions, trials were subdivided into "adapt" and "new" trials, depending on whether or not they were preceded by the same or the other condition (resulting in four regressors of interest). Neurons coding changes of the perceived size were expected to respond weaker in "adapt" compared with "new" trials and were subjected to a repeated-measures ANOVA with one factor, namely, Adaptation ("new" vs. "adapt").

Adaptation in the constant perceived size condition, intended to reveal size–distance invariant object representations, did not show any significant effect within the moon illusion network. Adaptation in the variable perceived size condition yielded significant activations in the middle occipital gyrus bilaterally. According to cytoarchitectonic probability maps (Eickhoff et al., 2005), both activations were located within area V3v, extending into V4 (see Table 1B and Figure 3B).

ROI Analysis

To investigate the relation between BOLD signal amplitudes and the perceived size of the moon, beta values were extracted from each local maximum within a cluster of activation associated with the moon illusion. This was done for each participant and for all four experimental conditions of Experiment 1.

To test whether perceived size predicted BOLD amplitudes, beta values and perceived size estimates were entered into simple linear regression analyses. When the moon was presented without a scene and at a lower position, perceived size was positively related to BOLD

amplitudes in right V1. Perceived size significantly predicted BOLD amplitudes and explained a significant portion of variance of BOLD amplitudes.

Importantly, when the moon was presented in the context of a scene and at a lowered position (i.e., when the moon's perceived size was increased), the perceived size of the moon significantly predicted BOLD amplitudes in left V1 as well as in left V3v and explained a significant amount of variance (see Table 2 and Figure 4).

DISCUSSION

The goal of our study was to reveal the brain regions involved in the moon illusion. To this end, we investigated the neural correlates of the moon illusion by means of fMRI and related these to the neural correlates of object size perception.

The behavioral data clearly indicated that the participants experienced the moon illusion during fMRI scanning: They perceived the moon as larger when it was presented at the lower position embedded in a 3-D scene compared with when it was presented at an elevated position within the same scene. Importantly, this effect did not occur as long as no scene was present. These findings replicate and extend previous behavioral studies in which the moon illusion was elicited by two-dimensional pictures (Jones & Wilson, 2009; Redding, 2002; Coren & Aks, 1990).

The moon illusion, as reflected by an interaction effect in the behavioral data, was accompanied by a significant interaction in the fMRI data. The latter was determined by comparing differential effects induced by both moon positions in the context of a scene with the respective position effects without a scene. This procedure allowed controlling for activations induced by the mere presence of the scene, as well as for those induced by position effects per se. The interaction term revealed neural activations bilaterally in primary visual cortex (around calcarine sulcus and lingual gyrus), in the left fusiform gyrus involving LOC, as well as in the right fusiform gyrus. The a priori predictions based on the illusion effect are straightforward. Brain areas involved in generating the moon illusion should exhibit strongest signal change patterns in the moon low condition. Likewise, retinotopic areas coding perceived size are expected to activate larger regions (i.e., stronger BOLD signal changes in regions coding increased perceived size) when the moon is perceived larger. This pattern was observed both in early visual areas

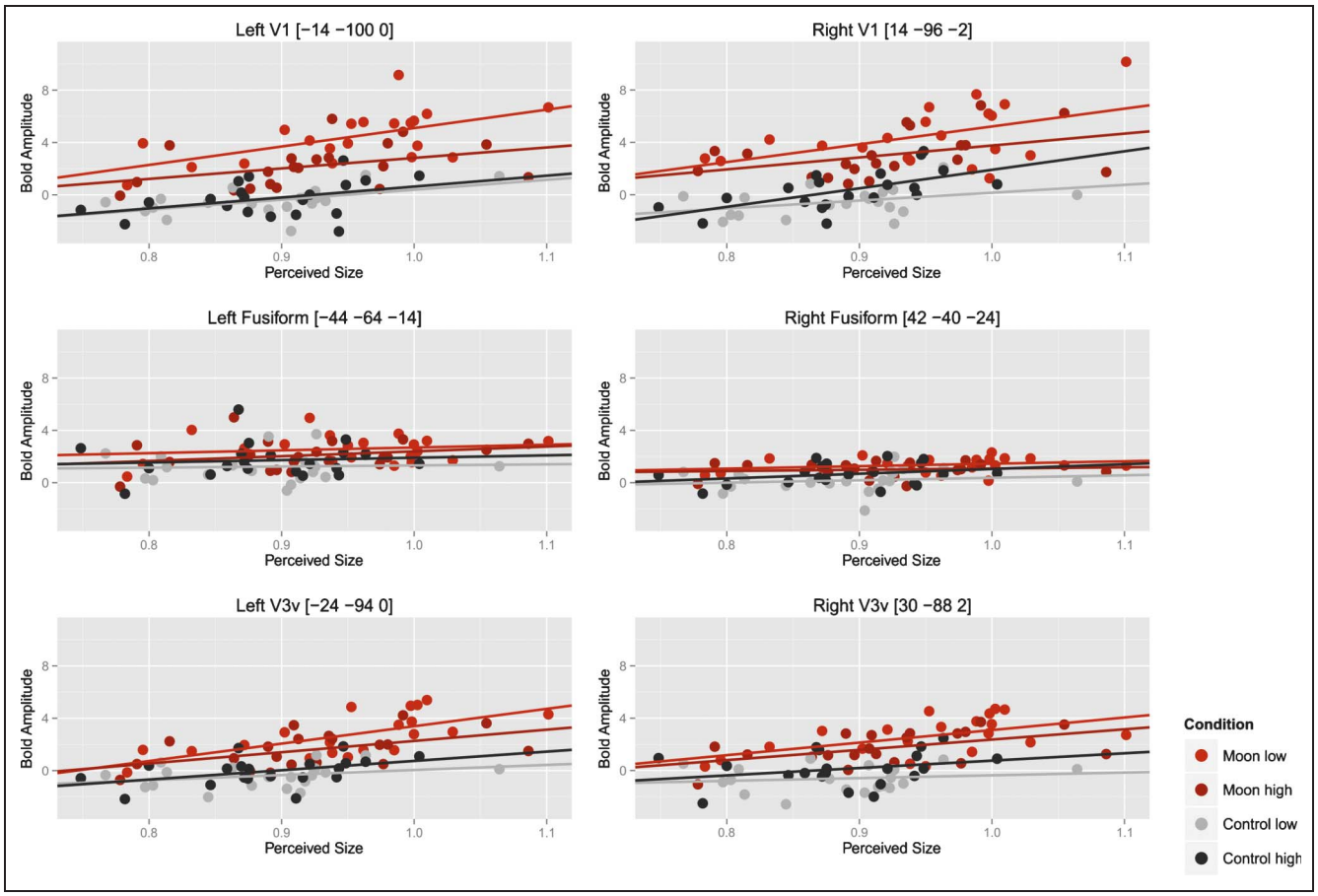

Figure 4. BOLD amplitudes observed in the different experimental conditions and in the different brain regions, presented as functions of perceived size.

as well as in higher tier ventral stream areas. These areas thus constitute the brain network involved in generating the moon illusion.

Experiment 2 further specified the functional role of these regions. Its variable perceived size condition allowed the determination of the brain areas that process changes of an object's perceived linear size when these changes were induced by manipulating its perceived depth.

V3v

Within the moon illusion network, bilateral V3v was found to be involved in recalculating an object's perceived size by taking into account its (perceived) distance. V3v, at least within the left hemisphere, showed increased BOLD amplitudes along with enlarged perceived moon sizes. In particular, this increase was only significant when the moon was presented within a scene and at a lowered position, indicating that size coding in left V3v was altered by the moon illusion.

These findings suggest that when the moon illusion was present (left), V3v not only responded stronger but also coded the moon's perceived size. Furthermore, as indicated by the results of Experiment 2, V3v was also involved in modifying perceived size based on distance information. These results implicate that (left) V3v contributes to the moon illusion by transforming angular size representations of the moon into linear size representations, taking into account distance information.

Fusiform Gyrus

BOLD amplitudes observed in the fusiform gyri were not linearly related to the perceived size of the moon. Nevertheless, activation patterns were influenced by scene context and moon position. More specifically, BOLD amplitudes were largest when a scene was present (as compared with when it was absent) and were modulated by the position of the moon. Accordingly, fusiform gyri were involved in processing scene context, but not in coding of the perceived moon size.

The fusiform gyri and lateral occipital areas are part of the ventral visual stream (Milner & Goodale, 1995; Goodale & Milner, 1992). They have been shown to be involved in coding and integrating object and context information (Altmann, Bülthoff, & Kourtzi, 2003). An integrated representation of a scene allows the combination of incoming information and the extraction of relative size contrasts as well as relative distances, both of which are relevant parameters for transforming angular to linear object size representations. These findings thus emphasize the role of ventral stream areas in generating the moon illusion and are in line with previous findings related to visual illusions (Plewan, Weidner, Eickhoff, & Fink, 2012; Weidner, Boers, Mathiak, Dammers, & Fink, 2010; Weidner & Fink, 2007; Brighina et al., 2003; Ritzl et al., 2003; Ffytche & Zeki, 1996).

V1

The V1 and V3v regions both showed a size-dependent modulation of activation and generally higher BOLD amplitude, when a lower moon was embedded into the scene.

Accordingly, the V1 region codes the perceived size changes as induced by the moon illusion. This finding is in good agreement with previous reports demonstrating an involvement of primary visual areas in coding visual size illusions (Sperandio, Chouinard, & Goodale, 2012; Song, Schwarzkopf, & Rees, 2011; Schwarzkopf, Song, & Rees, 2010; Fang, Boyaci, Kersten, & Murray, 2008). V1 constitutes the first cortical level of visual processing. Its involvement in the moon illusion thus provides evidence for theories advocating feed-forward mechanisms as one basic principle underlying the moon illusion.

However, the perceived size of the moon is altered by context information, which must be (spatially) integrated. Receptive fields of V1 neurons are relatively small and may not be able to sufficiently integrate information across areas that are large enough to induce the moon illusion (Smith, Singh, Williams, & Greenlee, 2001). Therefore, any modulation of perceived size in V1 most likely also depends on feedback information from higher visual areas (Weidner, Shah, & Fink, 2006; Lamme, Zipser, & Spekreijse, 2002; Lamme & Roelfsema, 2000). This view is supported by our finding that V1 in contrast to V3v is not directly involved in integrating retinal (angular) size and distance (as indicated by Experiment 2). Activation in V1 may thus depend on reentrant feedback signals originating in V3v.

The present data do not allow the assignment of these mechanisms to either pre- or postattentive levels of processing. Findings from behavioral studies suggest that apparent object size is coded relatively early. For instance, visual search studies investigating the Ebbinghaus illusion (Busch & Müller, 2004) reported evidence for a preattentive processing of apparent object size. In addition, it has been demonstrated that stimulus presentation for as short as 40 msec is sufficient to generate illusion induced modulations of manual response times in the Ponzo illusion (Plewan, Weidner, & Fink, 2012). Accordingly, the brain regions identified in this study are most likely involved in coding of size scaling at a preattentive level. This interpretation is consistent with Gregory's proposal concerning the moon illusion that the percept of the moon is enlarged by bottom–up scaling via depth clues present in the surrounding scene (Gregory, 2008).

Conclusion

In summary, the present data suggest that V3v constitutes a critical node, which transforms angular visual information to linear size information, presumably by taking into account parameters that are formed within the fusiform

gyri. Transformed linear size information is then fed back to the primary visual cortex.

These findings converge with recent fMRI, MEG, and TMS results related to other visual illusions (Plewan, Weidner, Eickhoff, et al., 2012; Mancini, Bolognini, Bricolo, & Vallar, 2011; Weidner et al., 2010; Weidner & Fink, 2007; Murray, Boyaci, & Kersten, 2006) and further extends them by strengthening the view that higher ventral stream areas play a major role in processing and generating context information, which then alters perceived object size in the context of visual illusions.

In line with theories suggesting that distance-based size scaling constitutes a relevant mechanism enlarging the perceived size of the moon (in the context of the moon illusion), the neural network underlying the moon illusion includes brain areas involved in recalculating perceived object size on the basis of retinal size and distance information.

Acknowledgments

R. W. was supported by the Deutsche Forschungsgemeinschaft (DFG, WE 4299/2-1). We are grateful to all our volunteers and our colleagues at the Institute of Neuroscience and Medicine, Research Center Jülich. Additional support to G. R. F. from the Marga- and Walter Boll Foundation is gratefully acknowledged.

Reprint requests should be sent to Ralph Weidner, Kognitive Neurowissenschaften, Institut für Neurowissenschaften und Medizin (INM-3), Forschungszentrum Jülich, Leo-Brandt-Str. 5, 52425 Jülich, Germany, or via e-mail: r.weidner@fz-juelich.de.

REFERENCES

Altmann, C. F., Bülthoff, H. H., & Kourtzi, Z. (2003). Perceptual organization of local elements into global shapes in the human visual cortex. *Current Biology, 13,* 342–349.

Ashburner, J., & Friston, K. (2005). Unified segmentation. *Neuroimage, 26,* 839–851.

Baird, J. C., Wagner, M., & Fuld, K. (1990). A simple but powerful theory of the moon illusion. *Journal of Experimental Psychology: Human Perception and Performance, 16,* 675–677.

Berkeley, G. (1709/1948). An essay toward a new theory of vision, 1709. In *Readings in the history of psychology* (pp. 69–80). East Norwalk, CT: Appleton-Century-Crofts.

Brighina, F., Ricci, R., Piazza, A., Scalia, S., Giglia, G., & Fierro, B. (2003). Illusory contours and specific regions of human extrastriate cortex: Evidence from rTMS. *European Journal of Neuroscience, 17,* 2469–2480.

Busch, A., & Müller, H. J. (2004). The Ebbinghaus illusion modulates visual search for size-defined targets: Evidence for preattentive processing of apparent object size. *Perception & Psychophysics, 66,* 475–495.

Coren, S., & Aks, D. J. (1990). Moon illusion in pictures: A multimechanism approach. *Journal of Experimental Psychology: Human Perception and Performance, 16,* 365–380.

Eickhoff, S. B., Stephan, K. E., Mohlberg, H., Grefkes, C., Fink, G. R., Amunts, K., et al. (2005). A new SPM toolbox for combining probabilistic cytoarchitectonic maps and functional imaging data. *Neuroimage, 25,* 1325–1335.

Enright, J. T. (1989). The eye, the brain, and the size of the moon: Toward a unified oculomotor hypothesis for the moon illusion. In M. Hershenson (Ed.), *The moon illusion* (pp. 59–121). Hillsdale, NJ: Erlbaum.

Fang, F., Boyaci, H., Kersten, D., & Murray, S. O. (2008). Attention-dependent representation of a size illusion in human V1. *Current Biology, 18,* 1707–1712.

Ffytche, D. H., & Zeki, S. (1996). Brain activity related to the perception of illusory contours. *Neuroimage, 3,* 104–108.

Friston, K. J., Holmes, A. P., Worsley, K. J., Poline, J. P., Frith, C. D., & Frackowiak, R. S. J. (1994). Statistical parametric maps in functional imaging: A general linear approach. *Human Brain Mapping, 2,* 189–210.

Gibson, J. J. (1979). *The ecological approach to visual perception*. Boston: Houghton Mifflin.

Gogel, W. C., & Mertz, D. L. (1989). The contribution of heuristic processes to the moon illusion. In M. Hershenson (Ed.), *The moon illusion* (pp. 235–258). Hillsdale, NJ: Erlbaum.

Goodale, M. A., & Milner, A. D. (1992). Separate visual pathways for perception and action. *Trends in Neurosciences, 15,* 20–25.

Gregory, R. L. (2008). Emmert's law and the moon illusion. *Spatial Vision, 21,* 3–5.

Grill-Spector, K., & Malach, R. (2001). fMR-adaptation: A tool for studying the functional properties of human cortical neurons. *Acta Psychologica, 107,* 293–321.

Hershenson, M. (1989). *The moon illusion*. Hillsdale, NJ: Erlbaum.

Jones, S. A., & Wilson, A. E. (2009). The horizon line, linear perspective, interposition, and background brightness as determinants of the magnitude of the pictorial moon illusion. *Perception & Psychophysics, 71,* 131–142.

Kaufman, L., & Kaufman, J. H. (2000). Explaining the moon illusion. *Proceedings of the National Academy of Sciences, 97,* 500–505.

Lamme, V. A., & Roelfsema, P. R. (2000). The distinct modes of vision offered by feedforward and recurrent processing. *Trends in Neurosciences, 23,* 571–579.

Lamme, V. A., Zipser, K., & Spekreijse, H. (2002). Masking interrupts figure-ground signals in V1. *Journal of Cognitive Neuroscience, 14,* 1044–1053.

Mancini, F., Bolognini, N., Bricolo, E., & Vallar, G. (2011). Cross-modal processing in the occipito-temporal cortex: A TMS study of the Müller-Lyer illusion. *Journal of Cognitive Neuroscience, 23,* 1987–1997.

McCready, D. (1986). Moon illusions redescribed. *Perception & Psychophysics, 39,* 64–72.

Milner, A. D., & Goodale, M. A. (1995). *The visual brain in action*. Oxford, UK: Oxford University Press.

Murray, S. O., Boyaci, H., & Kersten, D. (2006). The representation of perceived angular size in human primary visual cortex. *Nature Neuroscience, 9,* 429–434.

Neri, P., Bridge, H., & Heeger, D. J. (2004). Stereoscopic processing of absolute and relative disparity in human visual cortex. *Journal of Neurophysiology, 92,* 1880–1891.

Plewan, T., Weidner, R., Eickhoff, S. B., & Fink, G. R. (2012). Ventral and dorsal stream interactions during the perception of the Müller-Lyer illusion: Evidence derived from fMRI and dynamic causal modeling. *Journal of Cognitive Neuroscience, 24,* 2015–2029.

Plewan, T., Weidner, R., & Fink, G. R. (2012). The influence of stimulus duration on visual illusions and simple reaction time. *Experimental Brain Research, 223,* 367–375.

Redding, G. M. (2002). A test of size-scaling and relative-size hypotheses for the moon illusion. *Perception & Psychophysics, 64,* 1281–1289.

Restle, F. (1970). Moon illusion explained on the basis of relative size. *Science, 167,* 1092–1096.
Ritzl, A., Marshall, J. C., Weiss, P. H., Zafiris, O., Shah, N. J., Zilles, K., et al. (2003). Functional anatomy and differential time courses of neural processing for explicit, inferred, and illusory contours: An event-related fMRI study. *Neuroimage, 19,* 1567–1577.
Rock, I., & Ebenholtz, S. (1959). The relational determination of perceived size. *Psychological Review, 66,* 387–401.
Rock, I., & Kaufman, L. (1962). The moon illusion, II. *Science, 136,* 1023–1031.
Roscoe, S. N. (1989). The zoom-lens hypothesis. In M. Hershenson (Ed.), *The moon illusion* (pp. 31–58). Hillsdale, NJ: Erlbaum.
Ross, H., & Plug, C. (1998). The history of size constancy and size illusions. In V. Walsh & J. Kulikowski (Eds.), *Perceptual constancy: Why things look as they do* (pp. 499–528). New York: Cambridge University Press.
Ross, H., & Plug, C. (2002). *The mystery of the moon illusion*. Oxford, UK: Oxford University Press.
Schwarzkopf, D. S., Song, C., & Rees, G. (2010). The surface area of human V1 predicts the subjective experience of object size. *Nature Neuroscience, 14,* 28–30.
Smith, A. T., Singh, K. D., Williams, A. L., & Greenlee, M. W. (2001). Estimating receptive field size from fMRI data in human striate and extrastriate visual cortex. *Cerebral Cortex, 11,* 1182–1190.
Song, C., Schwarzkopf, D. S., & Rees, G. (2011). Interocular induction of illusory size perception. *BMC Neuroscience, 12,* 27.
Sperandio, I., Chouinard, P. A., & Goodale, M. A. (2012). Retinotopic activity in V1 reflects the perceived and not the retinal size of an afterimage. *Nature Neuroscience, 15,* 540–542.
Sperandio, I., Kaderali, S., Chouinard, P. A., Frey, J., & Goodale, M. A. (2013). Perceived size change induced by nonvisual signals in darkness: The relative contribution of vergence and proprioception. *The Journal of Neuroscience, 33,* 16915–16923.
Taylor, M. M., & Creelman, C. D. (1967). PEST: Efficient estimates on probability functions. *Journal of the Acoustical Society of America, 41,* 782–787.
Weidner, R., Boers, F., Mathiak, K., Dammers, J., & Fink, G. R. (2010). The temporal dynamics of the Müller-Lyer illusion. *Cerebral Cortex, 20,* 1586–1595.
Weidner, R., & Fink, G. R. (2007). The neural mechanisms underlying the Müller-Lyer illusion and its interaction with visuospatial judgments. *Cerebral Cortex, 17,* 878–884.
Weidner, R., Shah, N. J., & Fink, G. R. (2006). The neural basis of perceptual hypothesis generation and testing. *Journal of Cognitive Neuroscience, 18,* 258–266.